Thermally versus dynamically assisted Schwinger pair production

Greger Torgrimsson*

Theoretisch-Physikalisches Institut, Abbe Center of Photonics, Friedrich-Schiller-Universität Jena, Max-Wien-Platz 1, D-07743 Jena, Germany
and Helmholtz Institute Jena, Fröbelstieg 3, D-07743 Jena, Germany

(Received 4 March 2019; published 8 May 2019)

We study electron-positron pair production by the combination of a strong, constant electric field and a thermal background. We show that this process is similar to dynamically assisted Schwinger pair production, where the strong field is instead assisted by another coherent field, which is weaker but faster. We treat the interaction with the photons from the thermal background perturbatively, while the interaction with the electric field is nonperturbative (i.e., a Furry picture expansion in α). At $\mathcal{O}(\alpha^2)$ we have ordinary perturbative Breit-Wheeler pair production assisted nonperturbatively by the electric field. Already at this order we recover the same exponential part of the probability as previous studies, which did not expand in α. This means that we do not have to consider higher orders, so our approach allows us to calculate the preexponential part of the probability, which has not been obtained before in this regime. Although the prefactor is in general subdominant compared to the exponential part, in this case it can be important because it scales as $\alpha^2 \ll 1$ and is therefore much smaller than the prefactor at $\mathcal{O}(\alpha^0)$ (pure Schwinger pair production). We show that, because of the exponential enhancement, $\mathcal{O}(\alpha^2)$ still gives the dominant contribution for temperatures above a certain threshold, but, because of the small prefactor, the threshold is higher than what the exponential alone would suggest.

DOI: 10.1103/PhysRevD.99.096007

I. INTRODUCTION

Pure Schwinger pair production [1–3] by a constant electric field alone is unlikely to be observed any time soon, but there are nonspontaneous processes which have similar nonperturbative features and could occur at much lower intensities. One example is trident pair production $e^- \to 2e^- + e^+$ [4–12]. This requires much lower intensities because in the rest frame of a high-energy electron the field strength is much higher, and in the semiclassical regime this process has a similar nonperturbative exponential behavior as the Schwinger mechanism [4–6,10]. If one prefers to keep the initial state massless, one can instead significantly enhance the probability by sending a high-energy photon through the electric field [13]. Another way to enhance the probability is to add a second coherent field, which is weaker but faster [14]. The latter is referred to as dynamically assisted Schwinger pair production and has been studied in many papers in the past decade, see e.g., [14–22].

Another interesting question is how Schwinger pair production (and the effective action) is affected by a nonzero temperature, see e.g., [23–48]. It is fair to say that thermal pair production is a somewhat controversial topic with many papers that disagree with each other. In this paper we are interested in regimes where the thermal background leads to an exponential increase in the probability as in [41,43]. In this paper we only consider thermal photons. One might expect that effects from thermal fermions are suppressed at low temperatures, or one could imagine somehow filtering out the fermions [48], as we are only interested in the thermal distribution right before the field is applied. In any case, this is enough to study the exponential enhancement in [41,43], which we will show is very similar to dynamical assistance, by comparing with the approach in [19,20,22].

Since Schwinger pair production is nonperturbative in the field strength and since the additional weak field in dynamical assistance is also coherent, it might not have been obvious how the probability in dynamical assistance depends on the weak field. Even if not a nonperturbative dependence, one might have thought that one would in general have to calculate too many orders for an expansion in the field strength of the weak field to be useful. However, we have showed that it is in many cases useful to study dynamical assistance by such a power series expansion [19,20,22]. For the purpose of this paper, this is best

*greger.torgrimsson@uni-jena.de

illustrated with a weak field in the shape of a Sauter pulse. So, consider an electric field given by $E_z(t) = E(f_0(t) + \varepsilon f(t))$, where $E \ll 1$[1] and $f_0 = 1$ are the field strength and field shape of the strong and approximately constant field, and $\varepsilon \ll 1$ is the relative field strength of the weaker field. For a Sauter pulse we have $f(t) = 1/\cosh^2(\omega t)$. By treating both the strong and the weak field together with worldline instanton or WKB methods one finds a probability with the following exponential part [14]:

$$P \sim \exp\left\{-\frac{2}{E}\left(\frac{\sqrt{\gamma_*^2-1}}{\gamma_*^2} + \arcsin\frac{1}{\gamma_*}\right)\right\}, \tag{1}$$

where $\gamma_* = \gamma/\gamma_{\text{crit}}$, $\gamma = \omega/E$ is the Keldysh parameter and $\gamma_{\text{crit}} = \pi/2$. For $\gamma_* > 1$ this gives an exponential enhancement of the probability. Note that in those approaches this exponent is obtained from an expression that initially includes the field strength of the weak field, but the final result (1) is independent of ε. In [19] we showed that the exponent in (1) can also be obtained by treating the weak field perturbatively. In fact, we find this exponent already at the first order, i.e., from the absorption of a single photon from the weak field. We also showed that all the higher orders have the same exponential. Since the higher orders have higher powers of $\varepsilon \ll 1$ this means that the first order gives the dominant contribution for this field. The reason that this happens for a Sauter pulse can be understood from its Fourier transform, which at large Fourier frequencies scales as

$$f(\omega_1) \sim e^{-\frac{|\omega_1|}{\omega_*}} \tag{2}$$

for $|\omega_1| \gg \omega_*$ where $\omega_* = 2\omega/\pi$. This exponential decay is a slow decay, i.e., the Fourier transform is wide, which means that the suppression of the Fourier transform at large Fourier frequencies is less important than the suppression due to higher powers of the perturbative expansion parameter, so the first order gives the dominant contribution. The fact that we do not have to calculate higher orders of course makes the calculations simpler and we have found very good agreement with the exact numerical result [19]. From an experimental point of view it is important to notice that even if the characteristic frequency is well below the electron mass, $\omega \ll 1$, the Fourier frequencies that give the dominant contribution are on the order of the electron mass,

$$\omega_1^{\text{dom}} = 2\sqrt{1-\frac{1}{\gamma_*^2}} = \mathcal{O}(1). \tag{3}$$

While a Sauter pulse might not be the most realistic field shape, it is, as noted in [22], an example of a field which leads to the closest connection to thermally assisted pair production. In [41,43] the exponential part of the probability of pair production by a constant electric field at temperature T was obtained, and the result has exactly the same functional form as in (1) for dynamical assistance, but with $\gamma_* = 2T/E$. In this paper we will show that this close similarity means that we can study thermal assistance with essentially the same methods as the ones we used in [19,20,22] for dynamical assistance. Here it is the usual fine-structure constant $\alpha = e^2/(4\pi)$ that is the perturbative expansion parameter, so this is basically a Furry-picture expansion where the electric field is taken into account nonperturbatively. The first three terms are shown in Fig. 1. The zeroth order gives the usual Schwinger mechanism without any enhancement [27,31,32],[2] and the higher orders lead to exponential enhancement due to the absorption of thermal photons. In comparison with previous studies of the effective action, see e.g., [32], note that the nth order corresponds to $(n+1)$-loop diagrams. Note also that the thermal background describes the content of photons in the initial state, before the electric field is switched on.

FIG. 1. The first three terms in the Furry picture expansion. Double lines represent fermions dressed by the electric background field. Wiggly lines are photons from the thermal background.

The rest of this paper is organized as follows. In Secs. II–IV we calculate $\mathcal{O}(\alpha)$, $\mathcal{O}(\alpha^2)$ and higher orders, respectively. For $\mathcal{O}(\alpha)$ and $\mathcal{O}(\alpha^2)$ we calculate both the exponential and the prefactor part of the probability. In Sec. IV we show that the higher orders have the same exponential as $\mathcal{O}(\alpha^2)$, which means that we do not have to calculate the prefactor at higher orders.

II. FIRST ORDER

At first order we have pair production assisted by a single thermal photon, illustrated by the second diagram in Fig. 1. In dynamical assistance the exponent in (1) is generated by off-shell photons with zero spatial momentum. So, it seems already clear that a single on-shell thermal photon will not give (1). It is easy to check that it indeed gives something different. We start with the result in [13] for pair production by a single on-shell photon in a constant electric field, which is given by

$$P_\omega \sim \cdots \exp\left\{-\frac{2}{E}\left((1+p^2)\arctan\frac{1}{p} - p\right)\right\}, \tag{4}$$

[1]Throughout this paper we use units with $c = \hbar = m_e = k_B = 1$ and we rescale the field strength $eE \to E$, where m_e and e are the electron mass and charge.

[2]However, if one takes into account thermal fermions then the Pauli principle leads to a reduction of $\mathcal{O}(\alpha^0)$ [24,33,35,36,40,47].

where $p = |\sin\theta|\omega/2$, ω is the frequency of the photon, θ is the angle between the field and the direction in which the photon travels, and the ellipses denote the prefactor which can be found in [13]. As in [39], the probability of pair production by a single thermal photon is given by

$$P_1 = \sum_{\text{pol.}} \int \frac{\mathrm{d}^3\mathbf{k}}{(2\pi)^3} \frac{1}{e^{\omega/T}-1} P_\omega, \tag{5}$$

where $\mathbf{k}$ is the photon momentum and $1/(e^{\omega/T}-1)$ is the photon density. We need high frequencies for significant enhancement and we are interested in not too high temperature $T \ll 1$, so we can approximate $1/(e^{\omega/T}-1) \approx e^{-\omega/T}$ and perform the momentum integral with the saddle-point method. The exponent is maximized at $\theta = \pi/2$ and a frequency that is determined by a transcendental saddle-point equation [cf. Eq. (7) in [20]],

$$1 - p\arctan\frac{1}{p} = \frac{1}{\gamma}, \tag{6}$$

which we solve numerically and substitute in

$$P_1 = V_4 \frac{\alpha(\gamma E)^2}{8\pi} \frac{p(1+3p^2)}{\sqrt{\gamma-1}(\gamma-1-p^2)} e^{-\frac{2}{Ep}(1-\frac{1-p^2}{\gamma})}. \tag{7}$$

As shown in Fig. 2 this leads to a smaller exponential compared to (1), so its contribution to the probability is much smaller for $E \ll 1$. In the limit $\gamma \gg 1$ we find

$$P_1 \to V_4 \frac{\sqrt{3}\alpha T^2}{4\pi} \exp\left\{-\frac{8}{E\sqrt{3\gamma}}\right\}, \tag{8}$$

which vanishes in the limit $E \to 0$. [The exponential part of (8) has the same form as Eq. (9) in [20], but with $\gamma_{\text{crit}} = 1$]. Note that (8) is always nonperturbative in E, in contrast to the $\gamma \gg 1$ limit of (1), which scales as $e^{-2/T}$. Thus, the exponential scaling of P_1 is significantly different from (1).

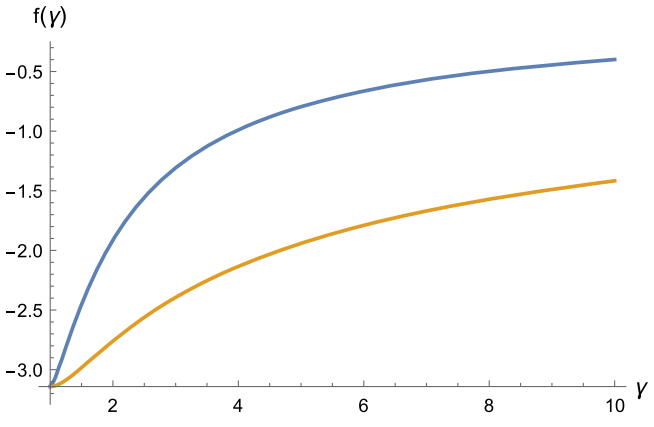

FIG. 2. Pair production probability $P \sim e^{f(\gamma)/E}$, where $\gamma = 2T/E$. The orange curve shows the exponent in (7) and the blue curve shows (1).

III. SECOND ORDER

At second order we have ordinary perturbative Breit-Wheeler pair production by two thermal photons assisted nonperturbatively by the electric field, illustrated by the third diagram in Fig. 1. Perturbative Breit-Wheeler at zero field was studied in [48][3] and the exponential part in the zero-temperature case was studied in [49]. As far as we are aware, this is the first time that the combination of both is studied. Here two photons are absorbed from the thermal background. While both are on shell their combined momentum can be off shell with zero spatial momentum, and this gives the dominant contribution. In [22] we showed how to calculate dynamical assistance at second order and higher. Here we can use essentially the same methods. This perturbative approach may in fact be even more useful here, because, while one in dynamical assistance can obtain the exact [$\mathcal{O}(\alpha^0)$] result by numerically solving the Dirac equation in both the strong and the weak field, see e.g., [18,21], there is no corresponding exact numerical approach for thermal assistance.

A. Derivation

The probability is given by (cf. [48,50] for the corresponding thermal sum in the purely perturbative case)

$$P_2 = \frac{1}{2}\sum_{\text{pol.}} \int \frac{\mathrm{d}^3\mathbf{k}_1}{(2\pi)^3} \frac{\mathrm{d}^3\mathbf{k}_2}{(2\pi)^3} \frac{1}{e^{\omega_1/T}-1} \frac{1}{e^{\omega_2/T}-1} \times \sum_{\text{spin}} \int \frac{\mathrm{d}^3\mathbf{p}}{(2\pi)^3} \frac{\mathrm{d}^3\mathbf{p}'}{(2\pi)^3} |M_2|^2, \tag{9}$$

where the factor of $1/2$ prevents double counting of identical particles, $\mathbf{k}_1$ and $\mathbf{k}_2$ are the momenta of the two photons, and $\mathbf{p}$ and $\mathbf{p}'$ are the momenta of the produced electron and positron, respectively. The amplitude can be written as

$$M_2 = \frac{(-ie)^2}{\sqrt{2\omega_1 2\omega_2}} \int \mathrm{d}^4x_1 \mathrm{d}^4x_2 \bar{u}_{s,\mathbf{p}}(t) e^{ip_j x_1^j} \not{\epsilon}_1 e^{-ik_1x_1} \times iG(x_1,x_2) \not{\epsilon}_2 e^{-ik_2x_2} v_{s',\mathbf{p}'}(t') e^{ip'_j x_2^j} + (1 \leftrightarrow 2), \tag{10}$$

where $\epsilon_\mu(\mathbf{k})$ denotes a polarization vector, $(1 \leftrightarrow 2)$ is obtained from the first term by swapping place of the two photons, and the electric field enters via the electron and positron spinors, u and v, and the propagator G. The exact propagator is given by [3,51,52]

[3]They also studied the thermal-field combination, but with a different method.

$$G(x,x') = -e^{-\frac{iE}{2}(z-z')(t+t')} \int \frac{\mathrm{d}^4q}{(2\pi)^4} e^{-iq(x-x')} \int_0^\infty \mathrm{d}s \times \exp\left\{-sm_\perp^2 + (q_0^2 - q_3^2)\frac{\tan(Es)}{E}\right\} \times [\not{q} + m + i(\gamma^0 q_3 + \gamma^3 q_0)\tan(Es)] \times [1 - i\gamma^0\gamma^3 \tan(Es)], \quad (11)$$

where $m_\perp = \sqrt{1+q_\perp^2}$ and $q_\perp = \{q_1, q_2\}$. The spinors can of course also be obtained exactly in a constant electric field, but here we only need the corresponding WKB approximations, which are given by (see e.g., [19,53,54])

$$U_r(t,\mathbf{q}) = (\gamma^0\pi_0 + \gamma^i\pi_i + 1)G^+(t,\mathbf{q})R_r$$
$$V_r(t,-\mathbf{q}) = (-\gamma^0\pi_0 + \gamma^i\pi_i + 1)G^-(t,\mathbf{q})R_r, \quad (12)$$

where $\pi_\perp = q_\perp$, $\pi_3(t) = q_3 - A(t)$, $\pi_0 = \sqrt{m_\perp^2 + \pi_3^2(t)}$, $r = 1, 2$, $\gamma^0\gamma^3 R_s = R_s$ and

$$G^\pm(t,\mathbf{q}) = [2\pi_0(\pi_0 \pm \pi_3)]^{-\frac{1}{2}} \exp\left[\mp i\int_0^t \mathrm{d}t'\pi_0(t')\right], \quad (13)$$

where the lower integration limit is arbitrary, and for a constant field we have

$$\int_0^t \pi_0 = -\frac{m_\perp^2}{2E}\left(\phi\left[\frac{p_3 - Et}{m_\perp}\right] - \phi\left[\frac{p_3}{m_\perp}\right]\right), \quad (14)$$

where

$$\phi(u) = u\sqrt{1+u^2} + \operatorname{arcsinh} u. \quad (15)$$

We start by performing the trivial spatial integrals. These give the overall momentum conservation $(2\pi)^2\delta^3(\mathbf{p} + \mathbf{p}' - \mathbf{k}_1 - \mathbf{k}_2)$ and another delta function which we use to perform the $\mathbf{q}$ integrals in the propagator. The square of the overall momentum delta function gives a spatial volume factor $V_3 = (2\pi)^3\delta^3(0)$ and a delta function which we use to perform the $\mathbf{p}'$ integrals. The s integral in the propagator receives the dominant contribution at $s = \mathcal{O}(E^0)$, so apart from the $e^{-\frac{iE}{2}(z-z')(t+t')}$ factor the propagator reduces to the field-free one. We can again approximate $1/(e^{\omega/T} - 1) \approx e^{-\omega/T}$. At the amplitude level we now have an exponential given by

$$e^{-\frac{\omega_1+\omega_2}{2T} + i\int_0^{t_1}\pi_0(\mathbf{p}) - i\omega_1 t_1 - iq_0(t_1-t_2) - i\omega_2 t_2 + i\int_0^{t_2}\pi_0(-\mathbf{p}')}. \quad (16)$$

We change variables $t_1 \to (m_\perp\tau_1 + p_3)/E$ and $t_2 \to (m'_\perp\tau_2 - p'_3)/E$, where $m'_\perp = \sqrt{1+p'^2_\perp}$, and to $\mathbf{\Sigma} = (\mathbf{k}_2 + \mathbf{k}_1)/2$ and $\mathbf{\Delta} = \mathbf{k}_2 - \mathbf{k}_1$. We perform the τ_i, q_0, $p_\perp$, $\mathbf{K}$ and $|\mathbf{\Delta}|$ integrals with the saddle-point method. We have a saddle point at $\tau_i = i/\gamma$, $q_0 = 0$, $p_\perp = 0$, $\mathbf{\Sigma} = 0$ and $|\mathbf{\Delta}| = 2\sqrt{1 - \frac{1}{\gamma^2}}$, where $\gamma = 2T/E$. This means that we are considering the region close to the point where the pair is produced without a heavier effective mass ($m_\perp = m'_\perp = 1$) by two photons colliding head on ($\mathbf{k}_2 = -\mathbf{k}_1$), and because the photons are assisted by the field, they have energies below the mass gap ($\omega_1 = \omega_1 = \sqrt{1 - \frac{1}{\gamma^2}} < 1$), but still close to it ($\omega_1 = \omega_2 \sim 1$). The perturbation around this point contributes to the prefactor. To calculate the spinor part of the prefactor we have used an explicit basis for γ^μ and R_r as in [19,22]. The summation over photon polarization can be done either by choosing explicit vectors ϵ_μ or as in the standard free-field case. In spherical coordinates for $\mathbf{\Delta}$ we find that the integral over the angle between $\mathbf{\Delta}$ and the electric field is elementary and the other angular integral is trivial. The integrand does not depend on p_3 so, as is well known, it then gives a temporal volume factor $\int \mathrm{d}p_3 = EV_0$.

As mentioned, for thermal assistance there are no exact numerical methods to compare with. However, in [19,20,22] we have showed that the corresponding (e.g., saddle-point) approximations for dynamical assistance agree well with the exact numerical result in the regimes that we are interested in here, and, because of the close similarity, those comparisons also give us a sense of the accuracy of the approximations presented here.

Another way to derive the same result is to use unitarity to obtain the pair production probability from loops with four photon vertices. Let $\mathcal{M}$ be the amplitude for two photons with $\mathbf{k}_1$, ϵ_1 and $\mathbf{k}_2$, ϵ_2 to scatter into two photons with $\mathbf{k}_3$, ϵ_3 and $\mathbf{k}_4$, ϵ_4. The zeroth order is given by $\mathcal{M}_0 = \delta_{13}\delta_{24} + \delta_{14}\delta_{23}$. The probability for this state to decay into a pair is given by

$$1 - \frac{1}{2}\sum_{3,4}(|\mathcal{M}_0|^2 + 2\mathrm{Re}\mathcal{M}_0^*\mathcal{M}_4) = -2\mathrm{Re}\mathcal{M}_4, \quad (17)$$

where $\mathcal{M}_4$ is illustrated Fig. 3. There is another overall factor of 2 that comes from the diagrams where the fermion loop goes in the opposite direction. In this approach the field dependence is expressed entirely in terms of the propagator (11), so we do not need the wave functions. Let s_i be the four s integration variables as shown in Fig. 3. The s_1 and s_3 integrals can be expanded around $s_1 = s_3 = 0$, as in the first approach. We rescale the remaining s variables $s_{2,4} \to s_{2,4}/E$, and then, before performing the $\mathbf{k}_1$ and $\mathbf{k}_2$ integrals, we have a saddle point at $s_2 = s_4 = \arccos\frac{\Sigma_\parallel}{\sqrt{1+\Sigma_\perp^2}}$, where $\Sigma_\mu = (k_1 + k_2)_\mu/2$ and $\Sigma_\parallel = \sqrt{\Sigma_0^2 - \Sigma_3^2}$. Let $\delta s_{2,4}$ be the perturbation around these saddle points. With $\delta s_+ = (\delta s_2 + \delta s_1)/2$ and $\delta s_- = \delta s_2 - \delta s_1$ we have

$$\exp\left\{\frac{1}{E}\left(-\frac{\Sigma}{\sqrt{1-\Sigma^2}}\frac{\delta s_-^2}{2} + 2\frac{\sqrt{1-\Sigma^2}}{\Sigma}\delta s_+^2\right)\right\}. \quad (18)$$

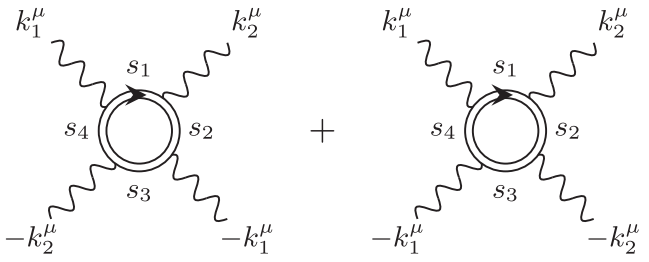

FIG. 3. The real part of these loops gives via unitarity the pair production probability.

The contour for the δs_+ integral starts along the real axis up to the saddle point, after which it turns into the imaginary direction. Since only the second half contributes to $\mathrm{Re}\mathcal{M}_4$, we have a factor of $1/2$ compared to a full Gaussian integral (cf. [22,55]).

If we in Fig. 3 connect the photon line with $-k_i^\mu$ to the one with k_i^μ, $i = 1, 2$, we find the same diagrams as if one replaces the free photon propagator with a thermal one which is obtained by adding an on-shell part (cf. e.g., [25]). This can help to relate our results to calculations of the effective action.

B. Results

Collecting everything we find

$$P_2 = V_4 \frac{\alpha^2(\gamma E)^3}{16\pi^2} \exp\left\{-\frac{2}{E}\left(\frac{\sqrt{\gamma^2-1}}{\gamma^2} + \mathrm{arccsc}\gamma\right)\right\} \times \frac{\sqrt{\gamma^2-1}(3\gamma^2-2) + (5\gamma^2-2\gamma^4-2)\mathrm{arccsc}\gamma}{\gamma(\gamma^2-1)^2\mathrm{arccsc}^2\gamma}, \quad (19)$$

where V_4 is a four-dimensional volume factor. The exponential part of (19) is exactly the same as the one found in [41,43] without expanding in α.[4] The exponential has the form in (19) for what [48] refers to as intermediate temperatures. As noted in [48], the prefactor in this regime had not been calculated before, so the prefactor in (19) is new. In deriving (19) we have assumed $\gamma > 1$ and, while the exponent has the expected limit as $\gamma \to 1$, i.e., $e^{-\pi/E}$, the saddle-point approximation of the prefactor breaks down in that limit. This is not a problem because P_2 is anyway small compared to P_0 for $\gamma \leq 1$, and as far as we are aware there are anyway no results for P_2 with $\gamma < 1$ that we could have compared with; the two-loop results in [32] correspond to P_1. The prefactor in a different parameter regime has been calculated in [46], but it has a nontrivial dependence on α and is therefore not something we can directly compare with.

However, there is a limit in which we can check the prefactor. For $\gamma \gg 1$ we expect, e.g., from comparing with similar results for dynamical assistance [19], to find a field independent result that agrees with what one finds by setting $E = 0$ from the start. This is indeed what we find,

$$P_2(\gamma \gg 1) = V_4 \frac{\alpha^2 T^3}{2\pi^2} e^{-\frac{2}{T}}, \quad (20)$$

which agrees with Eq. (8) in [48], see also [39], for ordinary perturbative Breit-Wheeler pair production summed over photons from a thermal background. On the one hand, it is quite natural that we recover the perturbative result, because $\gamma \gg 1$ can be obtained by keeping T fixed while taking $E \to 0$, and the exact P_2 should of course converge to the perturbative result as the field vanishes. On the other hand, the approximation of the integrals that leads to (19) is quite different from the way one would perform the corresponding integrals if $E = 0$ from the start, so this agreement is still an interesting and nontrivial check.

Equation (19) should be compared with the zeroth order, pure Schwinger result

$$P_0 = V_4 \frac{E^2}{4\pi^3} e^{-\frac{\pi}{E}}. \quad (21)$$

The exponent in P_2 gives an exponential enhancement as soon as $\gamma > 1$. However, P_2 has a much smaller prefactor because

$$\frac{\alpha^2 E^3}{16\pi^2}\left(\frac{E^2}{4\pi^3}\right)^{-1} \sim 4 \times 10^{-5} E < 10^{-5}, \quad (22)$$

so γ has to be sufficiently far above the threshold suggested by the exponent alone, so that the exponential enhancement can overcome the smaller prefactor to give something that is not just on the same order as P_0, but something significantly larger. On the other hand, P_2 quite quickly converges to its perturbative limit (20), so, if one wants something that is significantly different from perturbative Breit-Wheeler, γ cannot be too large. Figure 4 shows one example of this "window of significant difference," where P_2 is much larger than P_0 as well as its perturbative limit. In this example P_1 never gives the dominant contribution, because just above the threshold the exponential enhancement is not enough to compensate for the prefactor suppression compared to P_0, and for larger γ its exponent grows slower than P_2. These approximations suggest that if we let E be sufficiently large then P_1 could become important. However, it is not clear if our approximations are good for such a large E.

Another important point is that our perturbative approach allows us to see that the photons that give the dominant contribution have frequencies on the order of $\omega_{\mathrm{dom}} = \sqrt{1-\frac{1}{\gamma^2}} \lesssim 1$, i.e., on the order of the electron mass, even though the temperature is low, $T = E\gamma/2 \ll 1$. So, in this context, the distribution $1/(e^{\omega/T}-1)$ is good if it accurately describes the content of photons with energies on the

[4]Compare though with the WKB treatment in [41].

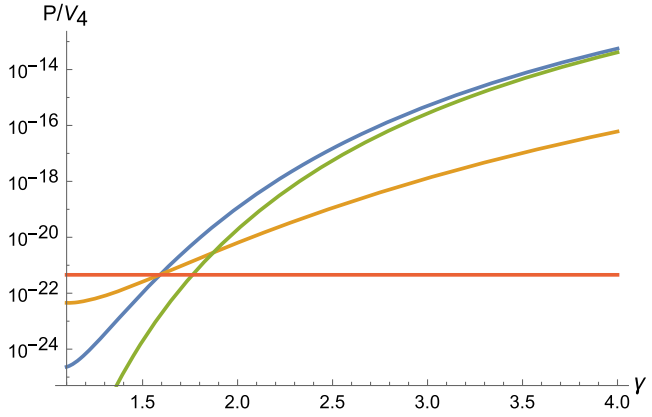

FIG. 4. Probability at $E = 0.08$. The red curve shows $\mathcal{O}(\alpha^0)$ (21), the orange curve shows $\mathcal{O}(\alpha)$ (7), the blue curve shows $\mathcal{O}(\alpha^2)$ (19) and the green curve shows its $\gamma \gg 1$ limit (20).

order of the electron mass. If the distribution instead falls off faster than $e^{-\omega/T}$, then one can expect a significant difference, as shown in [19,22] for dynamical assistance, where the dominant contribution can come from higher orders.

IV. HIGHER ORDERS

We showed in [19,22] for dynamical assistance that the dominant contribution can in general come from higher orders, but for a Sauter pulse all higher orders have the same exponential, namely the one in (1), which means that the first order gives the dominant contribution. In the case of thermal assistance we have just showed that the second order dominates over the first order for sufficiently weak fields. However, this is because here we are dealing with on-shell photons and the second order is the first order at which the total absorbed momentum can have zero spatial part, and it is the first order which is nonzero even without the electric field. At higher orders we can also have $\sum_{i=1}^{N} \mathbf{k}_i = 0$ and then the comparison with dynamical assistance suggests that higher orders should have the same exponential as P_2. To show this we use the approach in [22]. The starting point is

$$\begin{aligned} M_n &= (2\pi)^3 \delta^3\left(\mathbf{p} + \mathbf{p}' - \sum_{i=1}^{n} \mathbf{k}_i\right) e^n \mathfrak{A}_n \\ &\sim \int \mathrm{d}^4 x_1 \cdots \mathrm{d}^4 x_n \bar{u}(t_1) e^{ip_j x_1^j} \not{\epsilon}_1 e^{-ik_1 x_1} G(x_1, x_2) \\ &\quad \times \not{\epsilon}_2 e^{-ik_2 x_2} G(x_2, x_3) \cdots \not{\epsilon}_{n-1} e^{-ik_{n-1} x_{n-1}} \\ &\quad \times G(x_{n-1}, x_n) \not{\epsilon}_n e^{-ik_n x_n} v(t_n) e^{ip'_j x_n^j}. \end{aligned} \tag{23}$$

For $\sum_{i=1}^{N} \mathbf{k}_i = 0$ and $p_\perp = p'_\perp = 0$ we can obtain the exponential part by following the same steps as in [22]: We first perform the $\mathbf{x}_k$ integrals, which give delta functions, and we change variables $t_k \to (\tau_k + p_3)/E$. We expand all the s_k integrals around $s_k \sim 0$. We perform the integral over τ_1 and then the one over $q_1^{(1)}$ [momentum variable for $G(x_1, x_2)$], both with the saddle-point method. Then we perform the integrals over τ_2 and $q_0^{(2)}$, and so on. This gives

$$|M_n|^2 \sim \exp\left\{-\frac{2}{E}(\arccos\Sigma - \Sigma\sqrt{1-\Sigma^2})\right\}, \tag{24}$$

where $\Sigma = \frac{1}{2}\sum_{i=1}^{n} \omega_n$. The Boltzmann factor also only depends on this sum to leading order,

$$\prod_{i=1}^{n} \frac{1}{e^{\omega_n/T} - 1} \approx e^{-2\Sigma/T}. \tag{25}$$

Compare this with the WKB treatment in [41]. So, we can estimate the remaining integrals with the saddle point for this sum, $\Sigma_s = \sqrt{1 - \frac{1}{\gamma^2}}$, and then we find

$$P_n \sim \alpha^n \exp\left\{-\frac{2}{E}\left(\frac{\sqrt{\gamma^2 - 1}}{\gamma^2} + \operatorname{arccsc}\gamma\right)\right\}. \tag{26}$$

Thus, all higher orders have the same exponential as P_2. This means that P_2 gives the dominant contribution because the higher orders are suppressed by higher powers of α. Higher orders could be important if one has a thermal distribution that decays faster than the Boltzmann/exponential scaling, like for example a Gaussian decay. In some sense we are fortunate that the usual thermal distribution has this exponential decay, because it means that we only have to calculate the second order, and the exponential is exactly the same as the one previously obtained with different methods, which gives us a clear check.

V. CONCLUSIONS

We have studied thermally assisted Schwinger pair production by a Furry picture expansion in α. This has allowed us to use the perturbative methods we have developed in previous papers for dynamically assisted Schwinger pair production [19,20,22]. Apart from the fact that in thermal assistance one has an incoherent sum over photon modes, while in dynamical assistance one has a coherent sum, we have found that many aspects are very similar, especially for the case where the weak field in dynamical assistance is a time-dependent Sauter pulse, or some other pulse with exponentially decaying Fourier transform. The reason for this is that the Boltzmann distribution also has an exponential decay. In this context this is a wide distribution with a significant amount of high frequency modes. This means that already the absorption of one (in dynamical assistance) or two (in thermal assistance) photons from the background provides enough energy to give the dominant contribution. This is a good thing from a computational point of view, because it means that we can

calculate the preexponential factor without considering higher orders. The perturbative approach also shows that the photons that give the dominant contribution has energies on the order of the electron mass, even if the temperature is low. If one instead has a distribution that decays faster than an exponential, then the dominant contribution could come from higher orders.

In this paper we have considered a constant electric background field. We have found that $\mathcal{O}(\alpha^2)$ gives the dominant contribution above a certain threshold in γ. This threshold is a bit higher than what the exponential part alone would suggest, because the exponential enhancement first has to compensate for the prefactor which is much smaller than the one at $\mathcal{O}(\alpha^0)$. $\mathcal{O}(\alpha^2)$ should of course be larger than $\mathcal{O}(\alpha^0)$ and $\mathcal{O}(\alpha)$ for a sufficiently weak electric field, because the first two orders vanish without the field. The nontrivial conclusion is that $\mathcal{O}(\alpha^2)$ also gives the dominant contribution in a larger region with $\gamma \gtrsim 1$. It would be interesting to see how these results generalize to other field shapes, like for example a constant-crossed plane wave [39] or even a pulsed plane wave.

Another extension would be to consider initial states with thermal fermions in addition to thermal photons. Then at $\mathcal{O}(\alpha^0)$ one has the effect considered in [24,33,35,36,40,47], which leads to a suppression (for fermions) because of the Pauli principle. At $\mathcal{O}(\alpha^2)$ we would for example have thermal trident pair production, where a thermal fermion interacts with the electromagnetic background field and emits an intermediate photon which subsequently decays into an electron-positron pair. In this paper we have showed that the photons that give the dominant contribution have energies close to the electron mass, but their energies are still below the electron mass, which suggests that they should be more important than thermal fermions. However, the trident process can scale quadratically rather than linearly in the volume (see e.g., [4,5,9–11] for the zero-temperature constant-crossed plane wave case), so it would be interesting to study how large the trident contribution is compared to the $\mathcal{O}(\alpha^2)$ process considered here.

ACKNOWLEDGMENTS

G. T. thanks Holger Gies for inspiring and useful discussions and for reading and commenting on the manuscript, and Oliver Gould for interesting discussions. G. T. is supported by the Alexander von Humboldt foundation.

APPENDIX: STARTING POINT

In this Appendix we collect some well-known formulas (for textbooks see e.g., [56,57]), which one can use if one wants to derive (5) and (9) from the incoherent sum over all states weighted by the density matrix. In this paper we only consider thermal photons. A complete set for these states is given by

$$|\{n\}\rangle \coloneqq \prod_i \frac{(a_i^\dagger)^{n_i}}{\sqrt{n_i!}}|0\rangle, \tag{A1}$$

where i is an index for the momentum and polarization, n_i is the number of particles in the mode i, and the mode operators obey $[a_i, a_j^\dagger] = \delta_{ij}$. The system is put in a spatial volume V with periodic boundary conditions, which means as usual

$$\sum_i = V \sum_{\text{pol.}} \int \frac{\mathrm{d}^3\mathbf{k}}{(2\pi)^3}. \tag{A2}$$

The density matrix for the thermal ensemble is given by

$$\rho(\{n\}) = \langle\{n\}|\hat{\rho}|\{n\}\rangle = \prod_i \frac{e^{-n_i\omega_i/T}}{Z_i}, \tag{A3}$$

where the partition function is given by

$$Z_i = \frac{1}{1 - e^{-\omega_i/T}}. \tag{A4}$$

The photon field is given by

$$A^\mu(x) = \sum_i \frac{1}{\sqrt{2\omega_i V}} \epsilon_i^\mu a_i e^{-ikx} + \text{c.c.} \tag{A5}$$

The pair production probability is given by

$$\begin{aligned} P &= \sum_{\{n\}} \rho(\{n\}) \sum_{\{n'\}} \sum_{e^-e^+} |\langle\{n'\}; e^-e^+|S|\{n\}\rangle|^2 \\ &= \sum_{n=0}^{\infty} P_n, \end{aligned} \tag{A6}$$

where $P_n \propto \alpha^n$. At $\mathcal{O}(\alpha)$ and $\mathcal{O}(\alpha^2)$ this gives (5) and (9), respectively.

[1] F. Sauter, Über das Verhalten eines Elektrons im homogenen elektrischen Feld nach der relativistischen Theorie Diracs, Z. Phys. **69**, 742 (1931).

[2] W. Heisenberg and H. Euler, Consequences of Dirac's theory of positrons, Z. Phys. **98**, 714 (1936).

[3] J. S. Schwinger, On gauge invariance and vacuum polarization, Phys. Rev. **82**, 664 (1951).

[4] V. N. Baier, V. M. Katkov, and V. M. Strakhovenko, Higher-order effects in external field: pair production by a particle, Sov. J. Nucl. Phys. **14**, 572 (1972).

[5] V. I. Ritus, Vacuum polarization correction to elastic electron and muon scattering in an intense field and pair electro- and muoproduction, Nucl. Phys. **B44**, 236 (1972).

[6] C. Bamber *et al.*, Studies of nonlinear QED in collisions of 46.6-GeV electrons with intense laser pulses, Phys. Rev. D **60**, 092004 (1999).

[7] H. Hu, C. Muller, and C. H. Keitel, Complete QED Theory of Multiphoton Trident Pair Production in Strong Laser Fields, Phys. Rev. Lett. **105**, 080401 (2010).

[8] A. Ilderton, Trident Pair Production in Strong Laser Pulses, Phys. Rev. Lett. **106**, 020404 (2011).

[9] B. King and H. Ruhl, Trident pair production in a constant crossed field, Phys. Rev. D **88**, 013005 (2013).

[10] V. Dinu and G. Torgrimsson, Trident pair production in plane waves: Coherence, exchange, and spacetime inhomogeneity, Phys. Rev. D **97**, 036021 (2018).

[11] B. King and A. M. Fedotov, Effect of interference on the trident process in a constant crossed field, Phys. Rev. D **98**, 016005 (2018).

[12] F. Mackenroth and A. Di Piazza, Nonlinear trident pair production in an arbitrary plane wave: A focus on the properties of the transition amplitude, Phys. Rev. D **98**, 116002 (2018).

[13] G. V. Dunne, H. Gies, and R. Schützhold, Catalysis of Schwinger vacuum pair production, Phys. Rev. D **80**, 111301 (2009).

[14] R. Schützhold, H. Gies, and G. Dunne, Dynamically Assisted Schwinger Mechanism, Phys. Rev. Lett. **101**, 130404 (2008).

[15] M. Orthaber, F. Hebenstreit, and R. Alkofer, Momentum spectra for dynamically assisted Schwinger pair production, Phys. Lett. B **698**, 80 (2011).

[16] A. Otto, D. Seipt, D. Blaschke, B. Kämpfer, and S. A. Smolyansky, Lifting shell structures in the dynamically assisted Schwinger effect in periodic fields, Phys. Lett. B **740**, 335 (2015).

[17] M. F. Linder, C. Schneider, J. Sicking, N. Szpak, and R. Schützhold, Pulse shape dependence in the dynamically assisted Sauter-Schwinger effect, Phys. Rev. D **92**, 085009 (2015).

[18] C. Schneider and R. Schützhold, Prefactor in the dynamically assisted Sauter-Schwinger effect, Phys. Rev. D **94**, 085015 (2016).

[19] G. Torgrimsson, C. Schneider, J. Oertel, and R. Schützhold, Dynamically assisted Sauter-Schwinger effect—Nonperturbative versus perturbative aspects, J. High Energy Phys. 06 (2017) 043.

[20] G. Torgrimsson, C. Schneider, and R. Schützhold, Sauter-Schwinger pair creation dynamically assisted by a plane wave, Phys. Rev. D **97**, 096004 (2018).

[21] I. A. Aleksandrov, G. Plunien, and V. M. Shabaev, Dynamically assisted Schwinger effect beyond the spatially-uniform-field approximation, Phys. Rev. D **97**, 116001 (2018).

[22] G. Torgrimsson, Perturbative methods for assisted non-perturbative pair production, Phys. Rev. D **99**, 096002 (2019).

[23] W. Dittrich, Effective Lagrangians at finite temperature, Phys. Rev. D **19**, 2385 (1979).

[24] I. L. Bukhbinder, D. M. Gitman, and V. P Frolov, Density matrix for particle production processes in an external field, Sov. Phys. J. **23**, 529 (1980).

[25] P. H. Cox, W. S. Hellman, and A. Yildiz, Finite temperature corrections to field theory: Electron mass and magnetic moment, and vacuum energy, Ann. Phys. (N.Y.) **154**, 211 (1984).

[26] M. Loewe and J. C. Rojas, Thermal effects and the effective action of quantum electrodynamics, Phys. Rev. D **46**, 2689 (1992).

[27] P. Elmfors and B. S. Skagerstam, Electromagnetic fields in a thermal background, Phys. Lett. B **348**, 141 (1995); Erratum, Phys. Lett. B **376**, 330(E) (1996).

[28] J. Hallin and P. Liljenberg, Fermionic and bosonic pair creation in an external electric field at finite temperature using the functional Schrodinger representation, Phys. Rev. D **52**, 1150 (1995).

[29] A. K. Ganguly, J. C. Parikh, and P. K. Kaw, Thermal tunneling of q anti-q pairs in A-A collisions, Phys. Rev. C **51**, 2091 (1995).

[30] I. A. Shovkovy, One loop finite temperature effective potential in QED in the worldline approach, Phys. Lett. B **441**, 313 (1998).

[31] H. Gies, QED effective action at finite temperature, Phys. Rev. D **60**, 105002 (1999).

[32] H. Gies, QED effective action at finite temperature: Two loop dominance, Phys. Rev. D **61**, 085021 (2000).

[33] S. P. Gavrilov, D. M. Gitman, and J. L. Tomazelli, Density matrix of a quantum field in a particle-creating background, Nucl. Phys. **B795**, 645 (2008).

[34] S. P. Kim and H. K. Lee, Schwinger pair production at finite temperature in scalar QED, Phys. Rev. D **76**, 125002 (2007).

[35] S. P. Gavrilov and D. M. Gitman, One-loop energy-momentum tensor in QED with electric-like background, Phys. Rev. D **78**, 045017 (2008).

[36] S. P. Kim, H. K. Lee, and Y. Yoon, Schwinger pair production at finite temperature in QED, Phys. Rev. D **79**, 045024 (2009).

[37] A. Monin and M. B. Voloshin, Photon-stimulated production of electron-positron pairs in electric field, Phys. Rev. D **81**, 025001 (2010).

[38] S. P. Kim, H. K. Lee, and Y. Yoon, Nonperturbative QED effective action at finite temperature, Phys. Rev. D **82**, 025016 (2010).

[39] B. King, H. Gies, and A. Di Piazza, Pair production in a plane wave by thermal background photons, Phys. Rev. D **86**, 125007 (2012); Erratum, Phys. Rev. D **87**, 069905(E) (2013).

[40] K. Fukushima, Spectral representation of the particle production out of equilibrium—Schwinger mechanism in pulsed electric fields, New J. Phys. **16**, 073031 (2014).

[41] A. R. Brown, Schwinger pair production at nonzero temperatures or in compact directions, Phys. Rev. D **98**, 036008 (2018).
[42] L. Medina and M. C. Ogilvie, Schwinger pair production at finite temperature, Phys. Rev. D **95**, 056006 (2017).
[43] O. Gould and A. Rajantie, Thermal Schwinger pair production at arbitrary coupling, Phys. Rev. D **96**, 076002 (2017).
[44] M. Korwar and A. M. Thalapillil, Finite temperature Schwinger pair production in coexistent electric and magnetic fields, Phys. Rev. D **98**, 076016 (2018).
[45] P. Draper, Virtual and thermal Schwinger processes, Phys. Rev. D **98**, 125014 (2018).
[46] O. Gould, A. Rajantie, and C. Xie, Worldline sphaleron for thermal Schwinger pair production, Phys. Rev. D **98**, 056022 (2018).
[47] X. L. Sheng, R. H. Fang, Q. Wang, and D. H. Rischke, Wigner function and pair production in parallel electric and magnetic fields, Phys. Rev. D **99**, 056004 (2019).
[48] O. Gould, S. Mangles, A. Rajantie, S. Rose, and C. Xie, Observing thermal Schwinger pair production, arXiv: 1812.04089.
[49] P. Satunin, Breit-Wheeler pair production from worldline instantons, EPJ Web Conf. **191**, 02019 (2018).
[50] T. A. Weaver, Reaction rates in a relativistic plasma, Phys. Rev. A **13**, 1563 (1976).
[51] E. S. Fradkin, D. M. Gitman, and S. M. Shvartsman, *Quantum Electrodynamics with Unstable Vacuum*, Springer Series in Nuclear and Particle Physics (Springer, Berlin, 1991), p. 288.
[52] W. Dittrich and H. Gies, Probing the quantum vacuum. Perturbative effective action approach in quantum electrodynamics and its application, Springer Tracts Mod. Phys. **166**, 1 (2000).
[53] F. Hebenstreit, Schwinger effect in inhomogeneous electric fields, arXiv:1106.5965.
[54] F. Hebenstreit, R. Alkofer, and H. Gies, Schwinger pair production in space and time-dependent electric fields: Relating the Wigner formalism to quantum kinetic theory, Phys. Rev. D **82**, 105026 (2010).
[55] C. G. Callan, Jr. and S. R. Coleman, The fate of the false vacuum. 2. First quantum corrections, Phys. Rev. D **16**, 1762 (1977).
[56] L. Salasnich, *Quantum Physics of Light and Matter: Photons, Atoms, and Strongly Correlated Systems*, 2nd ed. (Springer, New York, 2017).
[57] F. Mandl and G. Shaw, *Quantum Field Theory*, 2nd ed. (Wiley, New York, 2010).